

OPEN ACCESS

**Repository of the Max Delbrück Center for Molecular Medicine (MDC)
in the Helmholtz Association**

<https://edoc.mdc-berlin.de/20421/>

Identification of the gliogenic state of human neural stem cells to optimize in vitro astrocyte differentiation

Alisch M., Kerkering J., Crowley T., Rosiewicz K., Paul F., Siffrin V.

This is the final version of the accepted manuscript. The original article has been published in final edited form in:

Journal of Neuroscience Methods
2021 SEP 01 ; 361(1): 109284
2021 JUL 07 (first published online: final publication)
doi: [10.1016/j.jneumeth.2021.109284](https://doi.org/10.1016/j.jneumeth.2021.109284)

Publisher: [Elsevier](https://www.elsevier.com)



Copyright © 2021 Elsevier Inc. All rights reserved. This manuscript version is made available under the Creative Commons Attribution-NonCommercial-NoDerivatives 4.0 International License. To view a copy of this license, visit <https://creativecommons.org/licenses/by-nc-nd/4.0/> or send a letter to Creative Commons, PO Box 1866, Mountain View, CA 94042, USA.

1 **Research Article**

2 **Title: Identification of the gliogenic state of human neural stem cells**
3 **to optimize in vitro astrocyte differentiation**

4 *Running title:* Optimizing in vitro human astrocyte differentiation

5 Marlen Alisch^{1#}, Janis Kerkering^{1#}, Tadhg Crowley¹, Kamil Rosiewicz¹, Friedemann Paul²,
6 Volker Siffrin^{1*}

7

8 ¹Neuroimmunology Lab, Experimental and Clinical Research Center (ECRC), Charité -
9 Universitätsmedizin Berlin und Max Delbrueck Center for Molecular Medicine, 13125 Berlin, Germany

10 ²Neurocure Clinical Research Center and Experimental and Clinical Research Center, Max Delbrueck
11 Center for Molecular Medicine and Charité - Universitätsmedizin Berlin, Corporate Member of Freie
12 Universität Berlin, Humboldt-Universität zu Berlin, and Berlin Institute of Health, 10117 Berlin,
13 Germany

14

15 #equal contribution

16

17 ***Address correspondence to:**

18 Volker Siffrin, Charité - Universitätsmedizin Berlin und Max-Delbrück-Centrum für Molekulare Medizin,
19 Berlin; Experimental and Clinical Research Center (ECRC), Lindenberger Weg 80, 13125 Berlin
20 Phone +49 . 30 . 450 540294 Fax: +49 . 30 . 450 540908 E-mail: volker.siffrin@charite.de

21

22 **Keywords**

23 astrocyte – H9 cells – human neural stem cells (hNSC) – SUZ12 – gliogenesis

24 **Highlights**

- 25
- The potential of glia differentiation increases with successive stem cell divisions
 - 26 • NSC, which underwent high cell divisions adopt a pre-glial cell phenotype
 - 27 • SUZ12, SMAD4 and STAT3 are potential upstream regulators of the gliogenic program
 - 28 • Targeted differentiation leads to pure mature and functional astrocyte cultures

29

30 **Abstract**

31 Background

32 Human preclinical models are crucial for advancing biomedical research. In particular
33 consistent and robust protocols for astrocyte differentiation in the human system are rare.

34 New Method

35 We performed a transcriptional characterization of human gliogenesis using embryonic H9-
36 derived hNSCs. Based on these findings we established a fast and highly efficient protocol for
37 the differentiation of mature human astrocytes. We could reproduce these results in induced
38 pluripotent stem cell (iPSC)-derived NSCs.

39 Results

40 We identified an increasing propensity of NSCs to give rise to astrocytes with repeated cell
41 passaging. The gliogenic phenotype of NSCs was marked by a down-regulation of stem cell
42 factors (e.g. SOX1 , SOX2 , EGFR) and an increase of glia-associated factors (e.g. NFIX ,
43 SOX9 , PDGFRa). Using late passage NSCs, rapid and robust astrocyte differentiation can
44 be achieved within 28 days.

45 Comparison with Existing Method(s)

46 In published protocols it usually takes around three months to yield in mature astrocytes. The
47 difficulty, expense and time associated with generating astrocytes in vitro represents a major
48 roadblock for glial cell research. We show that rapid and robust astrocyte differentiation can
49 be achieved within 28 days. We describe here by an extensive sequential transcriptome
50 analysis of hNSCs the characterization of the signature of a novel gliogenic stem cell
51 population. The transcriptomic signature might serve to identify the proper divisional maturity.

52 Conclusions

53 This work sheds light on the factors associated with rapid NSC differentiation into glial cells.
54 These findings contribute to understand human gliogenesis and to develop novel preclinical
55 models that will help to study CNS disease such as Multiple Sclerosis.

56

57 **1. Introduction**

58 Studying human neural cells in health and disease necessitates the development of diverse,
59 flexible and reproducible methods. The potential to differentiate stem cells, i.e. induced
60 pluripotent stem cells (iPSCs) of individual humans, into diverse cell types has allowed the
61 development of diverse human *in vitro* models for a whole host of organ systems and diseases
62 (Takahashi et al., 2007). However, *in vitro* models which focus on human neuroglial cells are
63 uncommon. According to current published standards, the generation of mature astrocytes

64 requires an *in vitro* differentiation time of over three months (Krencik et al., 2011; Roybon et
65 al., 2013). The difficulty, expense and time associated with generating astrocytes *in vitro*
66 represent a major roadblock for glial cell research.

67 NSCs—often referred to *in vivo* as neural progenitor cells (NPCs)—are multipotent cells with
68 the capacity to self-renew. In vertebrates these cells have been proposed as emerging in the
69 early neural plate (Temple, 2001) and mark the origin of neurogenesis and most gliogenesis
70 (apart from microglia). Mechanisms controlling neuronal and glial differentiation—aside from
71 being clearly tightly temporally regulated—are also sensitive to the extracellular environment
72 and paracrine factors as well as intrinsic regulatory mechanisms (Kessarar et al., 2001;
73 Temple, 2001). *In vivo*, it has been shown that the differentiation of glial cells occurs later than
74 the development of neurons (Bayer and Altman, 1991). This prompted researchers to model
75 these processes using systems biology and bioinformatic approaches (Qian et al., 2000),
76 wherein models explaining the timed generation of different cell subsets can be generalized
77 as either relying on extrinsic or intrinsic mechanisms. In extrinsic models, the potential of a
78 stem cell is similar in early and late divisions and the development of one population before
79 the other is driven by external cues that drive certain processes, e.g. signaling that promotes
80 neuronal differentiation over glial differentiation in the early phase. In intrinsic models the
81 potential of a stem cell changes over time, drawing support from the observation that most
82 cells from early divisions will develop into neurons, and cells from later phases are more likely
83 to give rise to glial cells.

84 *In vivo*, astrogenesis is regulated by both cell intrinsic mechanism such as epigenetic
85 chromatin modification and by extrinsic signals including growth factors and cytokines
86 (Hirabayashi and Gotoh, 2010; Namihira and Nakashima, 2013; Rowitch and Kriegstein,
87 2010). During astrocyte development in mice, late NPCs as well as early neurons release
88 cytokines such as CNTF (Bonni et al., 1997) and cardiotrophin 1 (CT1)(Barnabé-Heider et al.,
89 2005)—which activate the JAK/STAT signaling cascade—and LIF—which induces the
90 activation of BMP-SMAD pathways (Nakashima et al., 1999a). This leads to the expression of
91 STAT3 and SMAD (Nakashima et al., 1999b) inducing the expression of GFAP, S100B (He et
92 al., 2005) and NFIA, which in turn drives EAAT1 expression (Deneen et al., 2006) .

93 We illustrate here that repeated cell passaging drives antagonistic regulatory programmes for
94 gliogenic vs. neurogenic fate decision in hNSCs. Transcription factors for stemness are
95 downregulated along with those leading into the neuronal lineage, others involved in glial cell
96 differentiation are upregulated in a timed process, dependent on cell division, and in the
97 absence of external stimuli. Thus, we demonstrate that hNSC cultures *in vitro* recapitulate the
98 “neuron first, glia second” principle of differentiation by sequential activation of pro-neuronal,
99 anti-stemness and pro-glial programmes.

100 **2. Methods**

101 **2.1. Cell culture / Culturing neural stem cells**

102 Human Neural Stem Cells (hNSCs) derived from H9 hESCs were purchased from
103 ThermoFisher Scientific, Germany and cultivated according to the manufacturer's
104 recommendations. Cells were maintained in NSC-medium, consisting of KnockOut D-EM/F12
105 (Gibco-Thermo Fisher Scientific, Germany) supplemented with 2 mM Glutamax® (Gibco-
106 Thermo Fisher Scientific) 2 % StemPro Neural Supplement (Gibco-Thermo Fisher Scientific),
107 1% Penicillin-Streptomycin (Gibco-Thermo Fisher Scientific), 20 ng/μL bFGF (Peprotech,
108 Germany) and 20 ng/μL EGF (Peprotech, Germany) in a humidified incubator at 37° C and
109 with 5% CO₂.

110 **2.2. Astrocyte Differentiation**

111 For the differentiation of hNSCs to astrocytes, hNSCs were plated on Geltrex®- (Thermo
112 Fisher Scientific) coated plates in NSC-medium. When the cultures reached about 80 %
113 confluence, medium was switched to astrocyte differentiation media, which contains D-MEM
114 (Gibco-Thermo Fisher Scientific) supplemented with 2 mM Glutamax, 1 % N-2 (Thermo Fisher
115 Scientific), 1% Penicillin-Streptomycin, 1 % FCS (Sigma-Aldrich, Germany) and 20 ng/mL
116 CNTF (Miltenyi Biotec, Germany). Cells were cultivated for 3-12 weeks and passaged 3-5
117 times during differentiation. Medium was changed every 3-4 days.

118 **2.3. Immunofluorescence staining**

119 For immunofluorescence staining, astrocytes were seeded on Geltrex-coated Thermanox
120 coverslips (NUNC ThermoFischer Scientific). After differentiation immunofluorescence
121 stainings were performed for the astrocyte-associated markers GFAP (DAKO, Agilent,
122 Germany), S100B (Novus Biologicals, Centennial, USA), EAAT1 (Elabscience Houston, USA),
123 EAAT2 (Abcam, Germany), AQP4 (Elabscience), for neuronal stem cell marker NESTIN, the
124 proliferation marker KI67, and the neuronal marker MAP2 (all from Santa Cruz Biotechnology,
125 Germany). First, cells were fixed with 3.7 % paraformaldehyde (Santa Cruz Biotechnology)
126 and permeabilized using 0.1 % Triton® X-100 (Sigma-Aldrich, Germany). For staining
127 antibodies were diluted in 1 % bovine serum albumin (Sigma-Aldrich) in PBS and incubated
128 for 1 h at room temperature or overnight at 4 °C. After washing with PBS, cells were stained
129 with the corresponding secondary antibody; Alexa 488 anti-mouse (Invitrogen- ThermoFisher
130 Scientific) and Alexa 594 anti-rabbit (Invitrogen- ThermoFisher Scientific), each diluted 1:1000
131 in 1 % bovine serum albumin in PBS for 1 hour at room temperature. Cell nuclei were
132 counterstained with DAPI (Thermo Fisher Scientific) diluted 1:4000 and incubated for 10
133 minutes at room temperature. Samples were mounted with Fluorescence mounting Medium
134 (DAKO, Agilent) and evaluated using an inverted Leica DMI6000B microscope.

135 **2.4. Gene expression analysis**

136 For gene expression analysis total RNA was extracted using Quick-RNA™ MicroPrep (Zymo
137 Research, Germany) according to the manufacturer's protocol and isolated RNA was
138 transcribed to cDNA with High-Capacity RNA-to-cDNA™ Kit (Applied Biosystems-
139 ThermoFischer Scientific). Quantitative real time PCR was performed with QuantStudio™ 5
140 Real-Time PCR System (Applied Biosystems). One reaction consist of 10 µL of Fast SG qPCR
141 Master Mix, 0.24 µL ROX, 0.2 µL UNG, 2.56 µL RNase free water, all provided by Roboklon
142 (Germany), 4 µL of cDNA (2.5 ng/µL) and 1.5 µL forward and reverse primer. All primers are
143 listed in Table S2. *GAPDH*, *BACTIN* and *18sRNA* used as housekeeping genes and each
144 gene was processed in triplicate. For amplification the following thermocycler program was
145 executed: Stage 1: 37 °C, 2 min; 95 °C, 10 min; stage 2: 95 °C, 15 s; 60 °C, 60 s; stage 2 was
146 repeated for 40 cycles; stage 3 dissociation step.

147 **2.5. RNA-Sequencing analysis**

148 For sequencing analysis total RNA was isolated using Quick-RNA™ MicroPrep according to
149 the manufacturer's protocol. RNA quality control, library preparation and sequencing was
150 performed at Genomics Platform, MDC Berlin-Buch. For the construction of mRNA libraries
151 TruSeq RNA Library Prep (Illumina) was used. Single-Read 50bp sequencing was performed
152 on the HiSeq4000 platform (Illumina). The quality of the raw data was proofed with FastQC
153 (Andrews, S. (2010). FastQC: A Quality Control Tool for High Throughput Sequence Data,
154 online available, <http://www.bioinformatics.babraham.ac.uk/projects/fastqc/>) and filtered reads
155 were aligned against human reference transcriptome hg38 using Salmon (Patro et al., 2017)
156 Data analysis was carried out with the R/Bioconductor software package limma (Ritchie et al.,
157 2015). Genes with twofold differences and an adjusted $p < 0.01$ were defined as Differentially
158 Expressed Genes (DEGs). For analysis of Gene Ontology (GO) and KEGG pathway
159 enrichment Enrichr, a web database, was used (Chen et al., 2013).

160 **2.6. Glutamate uptake test**

161 For determination of the ability of astrocytes to take up glutamate, astrocytic medium was
162 replaced with fresh medium supplemented with PBS or 10 µM glutamate (1743, Carl Roth,
163 Karlsruhe, Germany) and incubated for 30 minutes at 37 °C. The supernatant of cell- and blank
164 wells, loaded with medium supplement with PBS or glutamate were analyzed with Glutamate-
165 Glo-Assay (J7021, Promega, Mannheim Germany) according to the manufacturer's
166 instruction. Luminescence was measured using a Tecan plate reader (Tecan, Männedorf) and
167 all values were normalized to the values of the negative control containing medium and PBS.

168 The change in glutamate concentration in cell supernatant was compared to non-cell
169 supernatant and determined using a titration-curve.

170 **2.7. Calcium imaging**

171 Astrocytes were cultured on black 96 well plates (Ibidi) and loaded with 1 μ M Fluo-4AM
172 (ThermoFischer Scientific) in FluoroBrite DMEM Media (ThermoFischer Scientific) for 20
173 minutes at 37 °C. Cells were then washed once with fresh medium and cells were allowed to
174 equilibrate for another 15 minutes. Fluorescence imaging was performed within an incubation
175 chamber at 37 °C, 5% CO₂ on an inverted Olympus Cell^R microscope (Olympus, Japan)
176 using an 20x/0.75 DIC objective and a mercury lamp with and 483/32 BP exciter filter.

177 Images were recorded by a Hamamatsu ImagEM CCD 9100-13 camera at 5-10 Hz for 3
178 minutes at 512 x 512 pixel resolution using the CellSense Imaging Software software ImageJ
179 was used for further processing.

180 **2.8. Induction of reactive astrocytes**

181 For the induction of reactive astrocytes, differentiated astrocytes were plated on Geltrex-
182 coated plates at a density of 100.000 cells/cm². After three days cells were cultivated in
183 astrocyte medium supplemented with 50 ng/mL TNFA (Miltenyi) and 10 ng/mL IL1B (200-01B,
184 Peprotech) for 48 h. After an incubation time of 48 h, cell lysis was performed, and RNA was
185 isolated. For gene expression analysis, the expression of complement component C3 was
186 compared between TNFA/IL1B treated experimental group and untreated control.

187 **2.9. Statistical analysis**

188 Statistical analysis was performed with GraphPad Prism (version 8.3.0). Significant differences
189 were determined using the non-parametric Mann-Whitney-Test, Kruskal-Wallis-Test.
190 Statistical significance was given when p-value < 0.05.

191 **3. Results**

192 **3.1. Targeted differentiation of human H9-derived NSCs leads to the generation of** 193 **mature and functional astrocytes**

194 For the differentiation of NSCs to astrocytes, NSCs were cultivated in DMEM based medium
195 supplemented with CNTF for at least 4 weeks with adaptations according to previously
196 published protocols (Shaltouki et al., 2013) (**Fig.1A**). To assess differentiation state, cultured
197 cells were characterized for the expression of astrocyte markers using rt-qPCR (**Fig.1B**). The
198 structural proteins GFAP and S100B are widely used canonical astrocyte markers. In addition,
199 we included genes coding for the water channel AQP4 and the aldehyde dehydrogenase
200 ALDH1L1, which are specifically expressed by mature astrocytes in the CNS as well as the

201 glutamate transporter EAAT1. Expression of all these markers was increased in differentiated
202 astrocytes compared to NSCs—*ALDH1L1* (20-fold), *AQP4* (16-fold) and *S100B* (17-fold)
203 were strongly upregulated, whereas *GFAP* (3-fold) and *EAAT1* (5-fold) were highly
204 upregulated in differentiated astrocytes as compared to undifferentiated NSCs.

205 Histological analysis further confirmed the astrocytic phenotype of differentiated NSCs
206 (**Fig.1C**). The majority of cells exhibited a protoplasmic astrocytic appearance, characterized
207 by numerous thick and short multibranched cytoplasmic processes. However, fibrous
208 astrocytes defined by longer, thinner, less numerous and less branched processes were also
209 detectable in differentiated astrocytes cultures (**Fig.1C**, upper left). Immunofluorescence
210 staining detected GFAP on the majority of cells and S100B, AQP4, EAAT1 and EAAT2 on
211 nearly all cells.

212 Next, we carried out a 3-pronged functional assessment of those cells that showed the typical
213 immunohistological markers of mature astrocytes. Astrocytes are known to be
214 electrophysiologically active CNS cells which show a spontaneous propagation of slow Ca^{2+}
215 waves, which are transmitted cell to cell by gap junctions (Cornell-Bell et al., 1990). Indeed,
216 we can confirm this wave-like spreading of Ca^{2+} across adjacent cells in the Calcium-dye Fluo-
217 4AM loaded NSCs derived astrocyte cultures (**Fig.1F** and **VideoS1**).

218 Furthermore, astrocytes are the main cell population responsible for removing glutamate from
219 the extracellular space, an essential process for CNS glutamate homeostasis and the
220 prevention of excitotoxic damage. We therefore assessed the ability of cultured H9-NSC-
221 derived astrocytes to remove glutamate from the supernatant of the cell cultures. Astrocytes
222 effected a 32 % clearance of glutamate from extracellular medium in comparison to the control
223 (**Fig.1D**).

224 Finally, astrocytes respond to inflammatory stimuli with an up-regulation of complement C3
225 (Liddelow et al., 2017). Treatment of the H9-NSC-derived astrocytes with TNFA (50 ng/ml) and
226 IL1B (10 ng/ml) for 24h induced a strong upregulation of complement C3 (39-fold) compared
227 to untreated astrocytes (**Fig.1E**).

228 **3.2. The potential of NSCs to differentiate into astrocytes increases with successive** 229 **stem cell divisions**

230 For basic propagation, H9-derived NSCs were passaged and maintained in stem cell medium
231 containing neural supplement and the growth factors EGF and bFGF. We primarily used
232 passages from 5 to 20 for our experiments. NSCs were passaged one to two times per week
233 in a ratio of 1:2 to 1:3. After observing the efficiency of astrocyte derivation from several
234 experiments, we suspected that the overall number of previous passages—and therefore the
235 number of cell divisions—might be a decisive factor for the observed differences in the
236 subsequent astrocyte differentiation periods. To investigate this effect of cellular division, we

237 focused on the characterization of the different NSCs passages, with higher passages naturally
238 undergoing more cellular division. We used passage 5 (NSCp5), passage 10 (NSCp10) and
239 passage 20 (NSCp20) NSCs for astrocyte differentiation.

240 First, we analyzed the morphology and the staining pattern for lineage specific markers.
241 Morphologically, NSCs changed from a compact cell in p5 to a more spine-like structure in p20
242 (**Fig. 2A**). Cultures were stained for the neural stem cell marker NESTIN and proliferation was
243 assessed by staining for the proliferation marker KI67. Notably, in NSCp5 almost all cells were
244 positive for NESTIN (99 %), slightly decreasing to 96 % in p10 and 92 % in p20 (**Fig. 2B**). The
245 expression of the proliferation marker KI67 decreased over time and the amount of KI-67
246 positive cells was lower in p10 (13 %) and p20 (22 %) compared to p5 (49 %). Most
247 interestingly, the expression of glial fibrillary acidic protein (GFAP)—a cytoskeletal protein
248 enriched in astrocytes but also adult neural stem cells (Yang and Wang, 2015)—significantly
249 increased between p5 and p10/p20 with 10 %, 63 % and 74 % GFAP positive cells in NSCp5,
250 NSCp10 and NSCp20 respectively (**Fig.2A and 2B**).

251 Next, we analyzed the timing of astrocyte differentiation when started with different passage
252 numbers in DMEM based medium supplemented with CNTF. In NSCp5 cultures after 28 days
253 of differentiation only a few isolated cells showed a strong expression for GFAP (**Fig. 2C**). For
254 NSCp5, it took between 56 and 70 days until a majority of cells stained positive for GFAP (81%
255 of all cells at day 70). When astrocyte differentiation was induced in NSCp10 after 42 days 96
256 % positive GFAP expressing cells were present, when starting with NSCp20, it took 28 days
257 to yield 95% positive GFAP cells. NSCp20 astrocyte differentiation was final after 28 days
258 based on our canonical marker set (see also below). NSCp20 showed an accelerated
259 differentiation as compared to NSCp5 (-42 days) and NSCp10 (-28 days) (**Fig. 2D**).

260 In summary, the higher the number of NSCs' divisions—as inferred by passage number—
261 before starting the differentiation, the shorter the time required to fully differentiate mature
262 astrocytes. Similarly, we observed faster astrocyte differentiation in higher divisional state
263 iPSC-derived NSC (**Fig.4 B-E**).

264 **3.3. Transcriptome analysis reveals that a higher number of cell divisions in NSCs leads** 265 **to an early glial phenotype**

266 To gain a clearer picture of the molecular differences underlying differential astrocyte
267 differentiation efficiency between NSCp5, NSCp10 and NSCp20, NSCs from these passages
268 were analyzed by next generation sequencing (NGS). For this, mRNA was purified from three
269 independent samples from NSCp5, NSCp10 and NSCp20 and from astrocytes which were
270 differentiated from these cells. Single-end 50bp sequencing was performed and data analysis
271 was performed with the R/Bioconductor software package limma (Ritchie et al., 2015). Genes

272 with more than two-fold change and adjusted P value <0.01 were termed DEGs (differentially
273 expressed genes).

274 Firstly, we assessed the expression of a list of *a priori* chosen markers of stemness and
275 differentiation towards glial and neuronal phenotypes (**Fig.3A**). The neuronal stem cell marker
276 *NESTIN*, *SOX1*, *SOX2*, *PAX6* and the stem cell marker *CDH2*—all present in NSCp5—were
277 gradually downregulated in NSCs with increasing passages. NSCs were maintained in medium
278 supplemented with bFGF and EGF over all passages. Expression of genes coding for the
279 receptor for EGF (*EGFR*) and as well receptor 1 for bFGF (*FGFR1*) were significantly
280 downregulated in NSCp20 whereas *FGFR4* significantly increased in NSCp20 compared to
281 NSCp5/10.

282 Furthermore, we investigated the expression of markers which are involved in the regulation
283 of stem cell fate decision, in particular *BHLHB2* from the Hes and ID family. *HES7* and *BHLHB2*
284 were significantly upregulated in NSCp20 compared to NSCp5/10. Further, the transcription
285 factors HES1-6 and ID1-4, which play a role in timing neuronal and glial differentiation by
286 repressing bHLH activators (Namihira and Nakashima, 2013; Yanagisawa et al., 2001), are
287 differentially expressed in NSCp5, NSCp10 and NSCp20.

288 Conversely, NSCp20 showed an upregulation of typical astroglia differentiation markers. The
289 NFI-family transcription factors (NFIA, NFIB, NFIX) as well as SOX9, which are highly
290 upregulated in NSCp20 compared to NSCp5/10, are important regulators of gliogenesis
291 (Cebolla and Vallejo, 2006; Kang et al., 2012). It is known that STAT3 and Notch-Signalling
292 play an essential role during astroglial differentiation (Kamakura et al., 2004; Tanigaki et al.,
293 2001), *STAT3*, *NOTCH1* and *NOTCH3* as well as the Notch receptors *DLK1* and *DNER* were
294 higher expressed in NSCp20 than in NSCp5/10. Moreover, we observed an increased
295 expression of the astrocyte differentiation factors *ATF3* and *ZBTB20*. NRSF acts as a
296 suppressor of neuronal differentiation (Gupta et al., 2009) and was significantly upregulated in
297 NSCp10 as compared to NSCp5. Furthermore, the expression of the astrocyte markers *CD44*,
298 *Vimentin*, *S100B*, *EAAT1* and *EAAT2* was increased in NSCp20 compared to p5/10.

299 Interestingly, markers for myelinating glial cells, e.g. *CNP*, *PLP1*, *CSPG4* and *PDGFRA*, were
300 also upregulated in NSCp20, indicating the more pro-glial and pan-glial propensity of
301 advanced passage NSCs. The neuronal marker *MAP2* was higher expressed in NSCp5
302 compared to NSCp10/20, whereas the neuronal marker *TUBB3* was higher in NSCp20
303 compared to NSCp5/10.

304 To confirm the results from the transcriptome analysis, we performed rt-qPCR analysis on
305 independent samples of NSCp5, NSCp10, NSCp20. As reference population, we used the
306 NSCp5. We evaluated the expression of distinct markers for stemness (*SOX2*, *NESTIN*),
307 astroglial progenitors (*ZBTB20*, *SOX9*, *NFIA*, *ATF3*) and mature astrocytes (*ALDH1L1*,
308 *EAAT1*, *S100B* and *GFAP*) (**Fig.3B**). The downregulation of stem cell marker *SOX2* could not

309 be confirmed and *NESTIN* showed only a trend to lower expression between NSCp20 and
 310 NSCp5/p10 in rt-qPCR. However, the astroglia differentiation marker *SOX9* was significantly
 311 increased in NSCp20 compared to p5 (10.9-fold), as well as *ZBTB20* (10.4-fold). There was
 312 also a trend of higher expression of *NFIA* (3.2-fold) and *ATF3* (2.5-fold) in NSCp20 compared
 313 to NSCp5/p10. The expression of *S100B* was highly increased in NSCp20 compared to p5
 314 and p10. Furthermore, *ALDH1L1* (6.1-fold) and *EAAT1* (3.1-fold) were also upregulated in
 315 NSCp20 compared to NSCp5.

316 In summary, with successive passaging NSCs undergo transcriptomic changes from a pan-
 317 neural stem cell to a glial progenitor cell type. We also checked a selected marker set derived
 318 from this analysis (*EGFR*, *FGFR1*, *FGFR4*, *HES7*, *ID1*, *ID3*, *ID4*, *SUZ12*, *STAT3*, *SOX1*,
 319 *SOX2*, *SOX9* and *NFIX*) in an iPSC line derived NSC population of early and late divisional
 320 state, which also suggests similar dynamics in iPSC derived NSCs (**Fig.4A**).

321 **3.4. Astrocytes generated from different NSC passages have similar phenotypes at the** 322 **end of differentiation**

323 In addition to comparing the transcriptome of different NSC passages we also compared the
 324 terminally differentiated astrocytes from each of the NSC passages to each other (**Fig.5A**).
 325 The duration of astrocyte differentiation varied depending on the passage of the source NSCs
 326 with NSCp5 taking 70 days, NSCp10 taking 42 days and NSCp20 achieving terminal astrocyte
 327 differentiation in 28 days. Principle component analysis of both the astrocyte and NSC cultures
 328 indicated that cultures of NSCp5 and NSCp10 showed a similar gene profile, astrocyte groups
 329 also clustered together, NSCp20s were distant from both NSCp5/NSCp10 and from all
 330 astrocytes (**Fig.5B**).

331 To identify the key genes involved in astrocyte differentiation and those changing with
 332 successive NSC proliferation, DEGs in a pair-wise comparison of NSCs and astrocytes were
 333 identified (**Fig.5C**). The results showed that more than 400 genes were upregulated and more
 334 than 300 were downregulated comparing NSCp5/NSCp10 vs. NSCp20. No DEGs were
 335 detected in the comparison of NSCp5 and NSCp10. Differentiated astrocytes and NSCs vary
 336 considerably in their gene expression. A range of 980 to 1407 genes were upregulated and
 337 between 771 to 1253 genes were significantly downregulated in astrocyte groups compared
 338 to their original NSC groups. Within the group of differentiated astrocytes, only few genes were
 339 differentially expressed depending on passage of the parent NSCs (astrocytes p5 vs. p20: 13
 340 up, 21 down; astrocytes p10 vs. p20: 10 up, 6 down).

341 The 50 most significantly differentially expressed genes (ranked by adjusted p value) are
 342 shown in a heatmap (**Fig.5D**). The expression profile of NSCp20 differed clearly from the
 343 profile of NSCp5/10 and from differentiated astrocytes. The top 50 regulated genes involved
 344 primarily transcription factors (e.g. *SOX9*, *NFIX*, *ID4*), as well as signaling molecules and

345 growth factors (for details see **Table S1**). The largest group of genes involved genes coding
 346 for cytoskeletal components, adhesion molecules and factors associated with extracellular
 347 matrix remodeling. Interestingly, there was also a set of genes involved in generation of
 348 bioactive retinoic acid (RA) derivatives, indicating that these cells might be a source of RA—
 349 indicated by their upregulation of *RDH10*—for developing neurons (Környei et al., 2007) while
 350 simultaneously becoming less receptive for RA (downregulation of *CRABP1*).

351 **3.5. Comparative transcriptomics reveal that NSCp20 adopt a pre-glial cell phenotype**

352 Next, we wanted to understand how the observed changes in gene expression fit with known
 353 signaling pathways and published gene ontologies (GO). Therefore, GO functional annotation
 354 and KEGG pathway enrichment analysis were performed with EnrichR database. We
 355 concentrated on identifying differential pathway regulation between NSCp5/p10s and
 356 NSCp20s (**Fig. 6**) and NSCp20s vs. astrocytes p5/p10/p20 (**Fig. 7**). The top 10 enriched GO
 357 terms for Biological Process (BP), Molecular Function (MF), Cellular Component (CC) and
 358 KEGG Pathways were identified.

359 Comparing NSCp5/10 to NSCp20, the top enriched GO terms for NSCp20 in the biological
 360 process category were extracellular matrix organization, axon guidance and axonogenesis.
 361 DEGs for NSCp5/10 scored high in excitatory synapse assembly, negative regulation of
 362 neurogenesis and nervous system development (**Fig.6A**). In the molecular function category,
 363 NSCp20 were enriched in collagen binding and glutamate receptor activity metabolism while
 364 the NSCp5/p10 did not turn up strongly regulated pathways (**Fig.6B**). The cellular component
 365 analysis showed mild enrichment of DEG in NSCp20 for integral component of plasma
 366 membrane, endoplasmic reticulum lumen and focal adhesion; NSCp5/p10 were slightly
 367 enriched in vesicle/granule related pathways (**Fig.6C**). The top 10 enriched KEGG pathways
 368 (**Fig.6D**) demonstrated that NSCp20 are enriched in ECM-receptor interaction, focal adhesion,
 369 PI3K-Akt-signalling and axon guidance; NSCp5/p10 turned up hardly any significantly
 370 regulated pathways compared to NSCp20. Analysis of potentially activated upstream
 371 transcription factors using EnrichR identified SUZ12 and SMAD4 (**Fig.6E**), which are known
 372 for controlling cell fate and division (Avery et al., 2010; Bracken et al., 2006). Furthermore, AR
 373 (androgen receptor)—which has been shown to be involved in myelination (Bielecki et al.,
 374 2016)—and PPAR δ —which is associated with maintenance of a neural progenitor cell status
 375 (Bernal et al., 2015)—were also potential regulators of the gene signature observed in
 376 NSCp20. The stemness and proliferation markers SOX2, NANOG and TCF3 were potential
 377 upstream effectors in NSCp5/p10. Potential protein–protein interactions were identified for
 378 upstream events of NSCp5/p10 vs. NSCp20 (**Fig.6F**), which included SMAD/STAT, key
 379 players in the regulation of BMP2 signaling pathway (Fukuda et al., 2007). Here, STAT3 and

380 FLI1 and UBTF, NCOA1, SPI1, FOXA1, CEBPB, SMAD1, SMAD2 and EP300 were identified
381 as relevant network potentially underlying the observed transcriptomic changes.

382 Taken together, in the course of NSC propagation—in particular in late passages—the
383 underpinnings of gliogenesis can be identified. These changes anticipate astrocytic function
384 and manifest with altered cytoskeletal, metabolic and proliferative states.

385 **3.6. Astrocyte differentiation drives membrane organization, matrix interaction and** 386 **receptor organization programs**

387 The transition of NSCp20 to astrocyte p5/p10/p20 further demonstrates the active role of
388 astrocytes in the complex functional tasks of glial cells. The top enriched Biological Process
389 GO term (**Fig.7A**) was 'nervous system development', which covers the process of progression
390 and formation of a mature nervous system. Extracellular matrix organization programmes were
391 enhanced in astrocytes as compared to NSCs, affirming the importance of shaping its cell type
392 specific environmental niche. The following enriched GO terms—cilium movement, synapse
393 assembly and neuron projection morphogenesis—are consistent with the tasks of seeking and
394 supporting developing neurons—one of the main functions of astrocytes. Simultaneously, the
395 transition of NSCs to astrocytes led to a major decrease in proliferation, shown by the
396 enrichment of cell cycle transition phases in NSCs.

397 In the category of Molecular Function (**Fig.7B**), collagen binding was the most enriched in
398 astrocytes as compared to NSCs and relative depletion was noticed in DNA-related processes,
399 i.e. proliferation related functions. The GO terms concerning cellular component identified
400 enrichment of DEGs related to membrane rafts and lysosome compartments in astrocytes and
401 a relative depletion of processes in chromosomal rearrangements (**Fig.7C**). This overall picture
402 was confirmed by the KEGG pathway analysis. Pathways related to the lysosome were found
403 to be enriched in NSCs, followed by ECM-receptor interaction, cell adhesion and axon
404 guidance. Again, cell cycle related pathways showed depletion in astrocytes compared to
405 NSCs (**Fig. 7D**).

406 Looking at predicted upstream transcription factors (**Fig. 7E**), SUZ12 was heavily implicated
407 in comparing astrocytes vs. NSCs and to a lesser extent in NSCp5/p10 vs. NSCp20. A strong
408 association was found for the transcription factor E2F4 with the NSCp20 (a co-transcription
409 factor for Smad3). Possible protein-protein interaction of transcription factors refer to
410 downregulated genes in the comparison of astrocytes vs. NSCp20. Here, three main factors
411 stand central in which NR0B1 and CEBPB were each linked to two separate clusters, yet both
412 factors are connected to E2F4 (**Fig 7F**).

413 To sum up the GO analysis, the transcriptome of NSCp20 is not just an intermediate state,
414 rather a gliogenic subtype of NSCs. The final differentiation of astrocytes associates with a
415 strong downregulation of proliferation related genes and networks. In tandem, astrocytes

416 upregulate a gene signature that indicates high interactivity with other CNS cell subsets, in
417 particular neurons, and the extracellular matrix.

418 **4. Discussion**

419 Here we show that NSCs' expression profile changes to a gliogenic phenotype with increasing
420 number of passages, which goes along with a downregulation of stem cell and neuronal
421 differentiation markers. Gene signature analysis identified *NFIX*, *SOX9*, *ID4*, *NOTCH* as well
422 as the potential upstream transcription factors SUZ12 and STAT3 to be key players in this
423 process. Expression of genes dependent on these transcription factors correlates with NSC
424 differentiation from a pan-neural to a gliogenic phenotype. Using this knowledge, we developed
425 a robust and efficient protocol to generate mature and functional astrocytes from human H9-
426 derived NSCs.

427 Several studies in recent years have contributed to the understanding of astrocyte
428 development in the CNS, which proceeds in a characteristic pattern; NPCs in rodents first
429 generate neurons and then give rise to glial cells (Qian et al., 2000). The sequential
430 development of neurons and astrocytes relies on a temporally-sensitive regulation of the
431 interplay between the intrinsic epigenetic status, transcriptions factors and environmental cues
432 (Hsieh and Gage, 2004; Schuurmans and Guillemot, 2002). We show in our experiments, that
433 proliferative embryonal derived human NSCs supplemented with bFGF and EGF
434 spontaneously develop a gliogenic phenotype after 20 passages. Compared to the process
435 described in rodents *in vivo*, the conversion of human NSCs into astrocytes followed a similar
436 pattern, i.e. a repeated cell passaging-associated switch from neurogenesis to gliogenesis.
437 Different hypotheses have been described to explain the sequential generation of different
438 CNS cell populations from NSCs (Qian et al., 2000). One assumption is that NSCs generate
439 in early divisions neuronal restricted progenitors and in later divisions glia restricted
440 progenitors. Alternatively, it is also conceivable that neuronal and glial progenitors are
441 randomly generated followed by a selection process exerted by external signals or conditions
442 that lead to the advantage of one population over the other. It remains to be checked if the
443 observed NSC phenotype development in our experiments is correlative (enrichment over time
444 due to extrinsic conditions) or instructive (following NSC intrinsic transcriptomic programs
445 dependent on cell cycling). This kind of question could be addressed by single cell sequencing
446 and pseudotime analysis to identify the relation of the diverse subpopulations in the NSC
447 cultures.

448 We cultivated NSCs over 5-20 passages in medium containing the growth factors EGF and
449 bFGF2 – an established strategy to maintain stem cell properties of NSCs (Kang et al., 2005;
450 Krampera et al., 2005). This may be important for the observed phase dependent change in
451 cell fate as previous studies have shown that high expression of EGFR enhanced astrogenesis

452 in precursor cells. Moreover, this receptor seems to segregate to daughter cells in an
453 asymmetrical way, leading to enhanced EGFR expression in daughter cells of differing fates,
454 co-expressing radial glia and astrocytic markers (Sun et al., 2001). In our study the expression
455 of *EGFR* was highest in NSCp10 followed by p5 and lowest in NSCp20. This indicates that
456 EGFR signaling might be an early event in the neural to gliogenic switch in NSC. Stem cell
457 defining transcription factors such as Sox1 and Sox2 have been shown to be critical for
458 maintaining stemness of NSC (Bylund et al., 2003; Graham et al., 2003). *SOX1* and *SOX2*
459 were progressively downregulated with increasing NSC passages indicating that this
460 downregulation can also contribute to a gliogenic rather than neurogenic phenotype. FGF2/
461 FGFR signaling has been identified as essential mitogenic factor in NPC biology (Yoshimura
462 et al., 2001) with FGFR1-4 having the potential to signal through different signaling pathways
463 (Hart et al., 2000). The partially contradictory effects of FGF2 signaling in NSCs —proliferative,
464 NSC-stabilizing (Lee et al., 2009), but also neurogenic (Yoshimura et al., 2001) and gliogenic
465 (Savchenko et al., 2019)—have not yet been elucidated, but might be explained by differences
466 in signal strength, differential expression of the different FGF receptors and/or context-
467 dependent other signals. Considering this, it is quite interesting to observe in our data the
468 progressive downregulation of *FGFR1* with increasing NSC passage paralleled by an
469 upregulation of *FGFR4*.

470 While neural and stem cell identity was lost with increasing NSC passaging, there was an
471 increase in gliogenic gene signature. Several signaling pathways have been described as
472 gliogenic, namely the JAK-STAT pathway (Bonni et al., 1997; He et al., 2005; Nakashima et
473 al., 1999b), the MAPK pathway (Yanagisawa et al., 2001), the activation of Notch (Ge et al.,
474 2002) and SMAD signaling (Fukuda et al., 2007; Gomes et al., 2003). In NSCp20 the
475 expression of *STAT3* was highly upregulated compared to NSCp5/10 and GO analysis
476 predicted *STAT3*, *SMAD1* and *SMAD3* to be involved in protein-protein interaction upstream
477 of upregulated genes. The overexpression of *Stat3* led to an increased number of astrocyte
478 progenitors (Hong and Song, 2014) and *Stat3* knockout mice exhibited a relative lack of white
479 matter astrocytes (Hong and Song, 2014). These findings and the results from our investigation
480 demonstrate that *STAT3* and *SMAD1* play an essential role in astrocyte differentiation.

481 Furthermore, *Stat3*, *Hes1* and *Hes5* interacts with Notch signaling, essential for differentiation
482 of astrocytes via the inhibition of stemness programs in NSCs (Kamakura et al., 2004). Notch
483 ligand *Dlk1* activates Notch signaling in Bergmann glia (Eiraku et al., 2002). In zebrafish, notch
484 ligand *Dner* inhibited NSC proliferation and induced glial and neuronal differentiation (Hsieh et
485 al., 2013). In our study, the expression of *HES1* and *HES5* decreased with the NSC passage
486 number. Furthermore, we observed an upregulation of *NOTCH* (*NOTCH1*, *NOTCH3*) and the
487 *NOTCH* ligands *DLK1* and *DNER* in NSCp20 compared to p5/10 indicating a switch from NSC
488 to astroglia differentiation.

489 In addition to the interaction with Notch and Stat3 leads via BMP2 to an activation of Smad1
490 (Fukuda et al., 2007) inducing a repression of neurogenesis and initiation of gliogenesis by
491 expression of basic Helix-Loop-Helix (bHLH) transcription factors from the ID and HES families
492 (Nakashima et al., 2001; Yanagisawa et al., 2001). We showed that the expression of *ID1*,
493 *ID2*, *ID3* as well as *HES2*, *HES6* and *HES7* were upregulated in NSCp20 compared to NSCp5.
494 Induced expression of *Id1* and *Id3* in murine neuroepithelial cells led to a downregulation of
495 the neuronal marker *Map2* (Nakashima et al., 2001), whereas an overexpression of *Id2* in
496 cortical progenitors completely inhibited the induction of neuron-specific genes (Toma et al.,
497 2000). In our work, we show that the expression of *ID4*, *HES1*, *HES4* and *HES5* were
498 downregulated in NSCp20 compared to NSCp5. Kondo et al. demonstrated that the expression
499 of *Id4* decreases over time as a form of internal clock that directs oligodendrocyte precursors
500 to a timed final differentiation (Kondo and Raff, 2000).

501 One of the most relevant players in the initiation of astrocyte differentiation is the transcription
502 factor nuclear factor-I (NFI) (Cebolla and Vallejo, 2006). We showed *NFIX*, *NFIB* and *NFIA*
503 expression to be significantly higher in NSCp20 as compared to NSCp5/10. In addition, the
504 transcription factor SOX9—strongly upregulated in NSCp20—has been shown to regulate the
505 induction of NFIA. Alternative ways to generate astrocytes have, e.g. employed transient
506 overexpression of NFIA in NSCs which resulted in astrocyte differentiation in a time frame of
507 56-77 days (Tchieu et al., 2019). *Sox9* knockout mice have an extended period of
508 neurogenesis coupled with a delay in the onset of oligodendrocyte differentiation (Stolt et al.,
509 2003). Both transcription factors are expressed at significantly higher levels in NSCp20, which
510 underwent a high number of divisions as compared to NSCp10 and NSCp5.

511 In our study, we identified SUZ12 as potential regulator of the observed NSCp5/10 to NSCp20
512 phenotype change. Bracken et al. could show that SUZ12 and other members of the PcG
513 group bind to promotor regions of genes of the Wnt, TGFB, FGF, Notch, and Hedgehog
514 signaling pathways known to be the regulators of developmental and differentiation processes
515 (Bracken et al., 2006; Zhang et al., 2019). The expression of the gene *SUZ12* was highest in
516 NSCp5/10, relatively downregulated in NSCp20s and lowest in differentiated astrocytes.

517 For final differentiation into astrocytes, NSCp20 were cultured in media with CNTF, a critical
518 activator of JAK-STAT pathways during astrocytogenesis (Barnabé-Heider et al., 2005; Bonni
519 et al., 1997). We observed that differentiated astrocytes do not proliferate anymore. This is
520 confirmed by the GO term analysis, which showed that genes associated with regulation of
521 cell cycle transition are downregulated in astrocytes compared to NSCs. For the
522 characterization of astrocytes we used a set of astrocyte structural markers, e.g. GFAP and
523 S100B, as well as the maturity markers ALDH1L1, EAAT1, EAAT2 and AQP4, which are most
524 often used astrocyte markers (Engel et al., 2016). It is to be said that astrocytes *in vivo* are a
525 heterogeneous cell population that are site and function specific. Their final use and task in the

526 brain, spinal cord or eye clearly sculpts their final profile of a mature astrocyte. Nevertheless,
527 most astrocyte populations share the above specific features. We use the commonly accepted
528 basic features of astrocytes to define our *in vitro* astrocytes in monocultures in distinction to
529 progenitors. This does, of course, not mean that we reduce astrocytes to these basic markers.
530 To sum up, we demonstrate that the transcriptome of the NSC changes with increasing
531 numbers of divisions. Transcription factors which suppress neurogenesis were upregulated in
532 NSCp20 and factors which maintain stem cell characteristics were downregulated in NSCp20
533 compared to p5/p10. This implies that both the suppression of neurogenic programs as well
534 as the initiation of gliogenic programmes occur in tandem during cultivation of NSCs.
535 Consequently, NSCs in p20 have a greater propensity to differentiate into mature astrocytes
536 in media supplemented with CNTF. The use of such a human astrocyte culture model enables
537 the more efficient investigation of the disease-specific role of astrocytes in human neurological
538 diseases such as Multiple Sclerosis and Neuromyelitis optica spectrum disorders.

539 **CRedit authorship contribution statement**

540 Marlen Alisch: Conceptualization, Methodology, Validation, Formal analysis, Investigation,
541 Writing - original draft, Writing - review & editing, Visualization. Janis Kerkerling: Methodology,
542 Validation, Formal analysis, Investigation, Writing - original draft, Writing - review & editing,
543 Visualization. Tadhg Crowley: Methodology, Validation, Formal analysis, Writing - review &
544 editing. Kamil Rosiewicz: Methodology, Investigation, Writing - review & editing. Friedemann
545 Paul: Writing - review & editing, Supervision, Project administration, Funding acquisition.
546 Volker Siffrin: Conceptualization, Methodology, Writing - original draft, Writing - review &
547 editing, Supervision, Project administration, Funding acquisition.

548 **Declaration of Competing Interest**

549 None.

550 **Acknowledgments**

551 We thank Jana Engelmann and Andrea Behm for expert technical support. Furthermore, we
552 thank the Berlin Institute of Health (BIH) Genomics Facility for support with NGS (Tatiana
553 Borodina) and the BIH Stem Cell Core Facility for generation of iPSCs (Norman Krüger,
554 Sebastian Diecke). This work was supported by the Gemeinnützige Hertie-Stiftung (to VS,
555 Hertie MyLab) and the German Research Foundation (Si-1886/1-1, Si-1886/3-1).

556

557 **5. Figure legends**

558 **Figure 1. Differentiation of NSC to fully characterized astrocytes**

559 **(A)** Schematic illustration of the differentiation of NSCs to astrocytes. After 4 to 10 weeks
 560 cultivation of NSC in media supplemented with CNTF and B27-supplement mature astrocytes
 561 are generated. **(B)** Quantitative rt-PCR analysis: expression of the astrocyte marker *ALDH1L1*,
 562 *EAAT1*, *GFAP*, *AQP4* and *S100B* in differentiated astrocytes compared to undifferentiated
 563 NSC (dotted line), * $p < 0.05$, $n = 3$. **(C)** Immunofluorescent characterization of NSC-derived
 564 mature astrocytes by antibody staining against GFAP, S100B, AQP4, EAAT1 and EAAT2. **(D)**
 565 Functional characterization by glutamate uptake test: In the presence of 10 μM glutamate in
 566 medium, astrocytes take up 32 % glutamate over 30 min, * $p < 0.05$, $n = 3$ (Mann-Whitney-U
 567 test). **(E)** After 24h treatment with TNFA (50 ng/ml) + IL1B (10 ng/ml), astrocytes show a
 568 significant increase of Complement factor C3 expression compared to untreated control which
 569 shows that astrocytes respond to inflammatory cytokines stimulation, * $p < 0.05$, $n = 4$ (Mann-
 570 Whitney-U test). **(F)** Astrocytes loaded with Flou-4AM show spontaneous wave-like Ca^{2+} -
 571 transients. **(G)** Images were recorded over 3 minutes at 7 Hz and ΔF of several single cells
 572 were shown.

573 **Figure 2. Differentiation of NSCp5, p10 and p20 to astrocytes**

574 **(A)** Expression of the neuronal stem cell marker NESTIN, the proliferation marker KI67 and
 575 the astrocyte marker GFAP in NSC p5, p10 and p20 representative for four independent
 576 experiments examined by immunofluorescence stainings (scale bar 50 μm) and **(B)** image
 577 analysis, * $p < 0.05$, $n=4$, (Kruskal-Wallis test). **(C)** NSC in p5, p10 and p20 were differentiated
 578 to astrocytes. After 0, 14, 28, 42, 56 and 70 days of differentiation the expression of the
 579 astrocytes marker GFAP was examined by immunofluorescence stainings representative for
 580 four experiments (scale bar 50 μm) and **(D)** image analysis was performed, * $p < 0.05$, ** $p <$
 581 0.01 , $n=4$ (Kruskal-Wallis test and Mann-Whitney-U test).

582

583 **Figure 3. NSCp5, NSCp10 and NSCp20 differ in the expression of stem cell, glial** 584 **developmental as well as astrocyte markers.**

585 **(A)** The heatmap shows the different expression of markers, which are associated with
 586 stemness, regulation of cell fate, astrogliogenesis, astrocytes, oligodendrocytes and neurons
 587 investigated by RNA-sequencing ($n=3$). Significantly regulated genes are written in bold
 588 ($p < 0.05$). **(B)** Quantitative rt-PCR analysis of independent samples shows the expression of
 589 selected stem cell, astrogliosis and astrocytes markers in NSCp5, NSCp10 and NSCp20, * $p <$
 590 0.05 , $n = 4$ (Kruskal-Wallis test).

591 **Figure 4. Analysis of neural stem cell and gliogenic markers in iPSC-derived NSCp5 and**
 592 **p17**

593 **(A)** Quantitative rt-qPCR analysis shows the expression of selected neural stem cell and
 594 gliogenic markers in iPSC-derived NSCp5 and NSCp17 **(B)** Immunofluorescent staining of the
 595 neuronal stem cell marker NESTIN, the proliferation marker KI67 and the astrocyte markers
 596 GFAP and AQP4 in iPSC-derived NSCp5 and NSCp17 before starting the differentiation to
 597 astrocytes and after 14 and 28 days of differentiation (scale bar 100 μ m).

598 **Figure 5. Analysis of differentially expressed genes in NSCp5, NSCp10, NSCp20 and**
 599 **differentiated astrocytes**

600 **(A)** Schematic illustration of experimental design. NSC were maintained in medium
 601 supplemented with bFGF and EGF over 20 passages. NSC from each passage were
 602 differentiated to astrocytes in media supplemented with CNTF. For transcriptome analysis
 603 RNA-sequencing was performed for NSCp5, NSCp10, NSCp20, Astrocytes-p5, Astrocytes-
 604 p10 and Astrocytes-p20 each in triplicates. **(B)** Principle Component Analysis of all samples
 605 shows that NSCp20 differ in their gene profile compared to NSCp5/p10 and differentiated
 606 astrocytes. **(C)** Numbers of differentially expressed genes (DEGs) among all sample in a pair-
 607 wise comparison (adjusted $p < 0.01$, fold change > 2) are shown in a histogram. **(D)** The
 608 heatmap shows the most significant differentially expressed genes (DEGs) among NSCp5,
 609 NSCp10, NSCp20, Astrocytes-p5, Astrocytes-p10 and Astrocytes-p20 (adjusted $p < 0.00001$,
 610 F-test).

611 **Figure 6. Gene ontology analysis of DEGs in NSCp5/p10 versus NSCp20**

612 **(A-D)** Gene ontology analyses (GO) show functional transition from NSCp5/p10 to NSCp20
 613 and involved pathways. The 10 most significant GO for Biological Process **(A)**, Molecular
 614 Function **(B)**, Cellular Component **(C)** and the top 10 most significant biological pathways **(D)**
 615 associated with upregulated and downregulated genes in NSCp20 versus NSCp5/p10 are
 616 depicted. **(E-F)** Examination of consensus target genes for transcription factors and protein-
 617 protein-interaction for the transcription factors in NSCp20 compared to NSCp5/p10. **(E)**
 618 Transcription Factors upstream which are associated with up and downregulated genes. **(F)**
 619 Protein-Protein-Interaction for upstream transcriptions factors (only significant interactions are
 620 shown).

621 **Figure 7. GO analysis of DEGs in NSCp20 versus mature astrocytes (p5/p10/p20)**

622 **(A-D)** GO analysis show functional transition from NSCp20 and differentiated astrocytes
 623 (p5/p10/p20) involved pathways. The 10 most significant GO for Biological Process **(A)**,
 624 Molecular Function **(B)**, Cellular Component **(C)** and the top10 significant biological pathways
 625 **(D)** associated with upregulated and downregulated genes in NSCp20 versus NSCp5/p10 are

626 depicted. **(E-F)** Examination of consensus target genes for transcription factors and protein-
 627 protein-interaction for the transcription factors in NSCp20 compared to NSCp5/p10. **(E)**
 628 Transcription Factors upstream which are associated with up and downregulated genes and
 629 **(F)** Protein-Protein-Interaction for upstream transcriptions factors (only significant interaction
 630 are shown).

631 **Appendix/ Supplementary data**

632 **Table S1**

633 Overview of the top 50 differentially expressed genes among NSCp5, NSCp10, NSCp20,
 634 Astrocytes-p5, Astrocytes-p10 and Astrocytes-p20 (adjusted $p < 0.00001$, F-test). Genes are
 635 categorized upon their primary function. Examples of specific functions influencing the
 636 nervous system are depicted and referred to their original publication.

637 **Table S2**

638 List of primers and corresponding sequence used for quantitative rt-PCR analysis.
 639 FWD: Forward primer. REV: reverse primer.

640 **Video S1**

641 Astrocytes were cultured on black 96 well plates (Ibidi) and loaded with 1 μ M Fluo-4AM
 642 (ThermoFischer Scientific) in FluoroBrite DMEM Media (ThermoFischer Scientific) for 20
 643 minutes at 37 °C. Cells were washed once with fresh medium and cells were allowed to
 644 equilibrate for another 15 minutes. Fluorescence imaging was performed within an incubation
 645 chamber at 37 °C, 5% CO₂ on an inverted Olympus Cell[^]R microscope (Olympus, Japan)
 646 using a 20x/0.75 DIC objective and a mercury lamp with and 483/32 BP exciter filter.
 647 Images were recorded by a Hamamatsu ImagEM CCD 9100-13 camera at 5-10 Hz for 5
 648 minutes at 512 x 512 pixel resolution using the CellSense Imaging Software. ImageJ was used
 649 for further processing.

650 **References**

- 651 Avery, S., Zafarana, G., Gokhale, P.J., Andrews, P.W., 2010. The Role of SMAD4 in Human
 652 Embryonic Stem Cell Self-Renewal and Stem Cell Fate. *STEM CELLS* 28, 863–873.
 653 <https://doi.org/10.1002/stem.409>
- 654 Barnabé-Heider, F., Wasylnka, J.A., Fernandes, K.J.L., Porsche, C., Sendtner, M., Kaplan,
 655 D.R., Miller, F.D., 2005. Evidence that embryonic neurons regulate the onset of cortical

- 656 gliogenesis via cardiotrophin-1. *Neuron* 48, 253–265.
657 <https://doi.org/10.1016/j.neuron.2005.08.037>
- 658 Bayer, S.A., Altman, J., 1991. *Neocortical development*. Raven Press, New York.
- 659 Bernal, C., Araya, C., Palma, V., Bronfman, M., 2015. PPAR β/δ and PPAR γ maintain
660 undifferentiated phenotypes of mouse adult neural precursor cells from the
661 subventricular zone. *Front. Cell. Neurosci.* 9. <https://doi.org/10.3389/fncel.2015.00078>
- 662 Bielecki, B., Mattern, C., Ghoumari, A.M., Javaid, S., Smietanka, K., Abi Ghanem, C., Mhaouty-
663 Kodja, S., Ghandour, M.S., Baulieu, E.-E., Franklin, R.J.M., Schumacher, M., Traiffort,
664 E., 2016. Unexpected central role of the androgen receptor in the spontaneous
665 regeneration of myelin. *Proc. Natl. Acad. Sci. U. S. A.* 113, 14829–14834.
666 <https://doi.org/10.1073/pnas.1614826113>
- 667 Bonni, A., Sun, Y., Nadal-Vicens, M., Bhatt, A., Frank, D.A., Rozovsky, I., Stahl, N.,
668 Yancopoulos, G.D., Greenberg, M.E., 1997. Regulation of gliogenesis in the central
669 nervous system by the JAK-STAT signaling pathway. *Science* 278, 477–483.
670 <https://doi.org/10.1126/science.278.5337.477>
- 671 Bracken, A.P., Dietrich, N., Pasini, D., Hansen, K.H., Helin, K., 2006. Genome-wide mapping
672 of Polycomb target genes unravels their roles in cell fate transitions. *Genes Dev.* 20,
673 1123–1136. <https://doi.org/10.1101/gad.381706>
- 674 Bylund, M., Andersson, E., Novitsch, B.G., Muhr, J., 2003. Vertebrate neurogenesis is
675 counteracted by Sox1-3 activity. *Nat. Neurosci.* 6, 1162–1168.
676 <https://doi.org/10.1038/nn1131>
- 677 Cebolla, B., Vallejo, M., 2006. Nuclear factor-1 regulates glial fibrillary acidic protein gene
678 expression in astrocytes differentiated from cortical precursor cells. *J. Neurochem.* 97,
679 1057–1070. <https://doi.org/10.1111/j.1471-4159.2006.03804.x>
- 680 Chen, E.Y., Tan, C.M., Kou, Y., Duan, Q., Wang, Z., Meirelles, G.V., Clark, N.R., Ma'ayan, A.,
681 2013. Enrichr: interactive and collaborative HTML5 gene list enrichment analysis tool.
682 *BMC Bioinformatics* 14, 128. <https://doi.org/10.1186/1471-2105-14-128>
- 683 Cornell-Bell, A.H., Finkbeiner, S.M., Cooper, M.S., Smith, S.J., 1990. Glutamate induces
684 calcium waves in cultured astrocytes: long-range glial signaling. *Science* 247, 470–
685 473. <https://doi.org/10.1126/science.1967852>
- 686 Deneen, B., Ho, R., Lukaszewicz, A., Hochstim, C.J., Gronostajski, R.M., Anderson, D.J.,
687 2006. The transcription factor NFIA controls the onset of gliogenesis in the developing
688 spinal cord. *Neuron* 52, 953–968. <https://doi.org/10.1016/j.neuron.2006.11.019>
- 689 Eiraku, M., Hirata, Y., Takeshima, H., Hirano, T., Kengaku, M., 2002. Delta/notch-like
690 epidermal growth factor (EGF)-related receptor, a novel EGF-like repeat-containing
691 protein targeted to dendrites of developing and adult central nervous system neurons.
692 *J. Biol. Chem.* 277, 25400–25407. <https://doi.org/10.1074/jbc.M110793200>
- 693 Engel, M., Do-Ha, D., Muñoz, S.S., Ooi, L., 2016. Common pitfalls of stem cell differentiation:
694 a guide to improving protocols for neurodegenerative disease models and research.
695 *Cell. Mol. Life Sci. CMLS* 73, 3693–3709. <https://doi.org/10.1007/s00018-016-2265-3>
- 696 Fukuda, S., Abematsu, M., Mori, H., Yanagisawa, M., Kagawa, T., Nakashima, K., Yoshimura,
697 A., Taga, T., 2007. Potentiation of Astroglialogenesis by STAT3-Mediated Activation of

- 698 Bone Morphogenetic Protein-Smad Signaling in Neural Stem Cells. *Mol. Cell. Biol.* 27,
699 4931–4937. <https://doi.org/10.1128/MCB.02435-06>
- 700 Ge, W., Martinowich, K., Wu, X., He, F., Miyamoto, A., Fan, G., Weinmaster, G., Sun, Y.E.,
701 2002. Notch signaling promotes astroglial lineage commitment via direct CSL-mediated glial gene
702 activation. *J. Neurosci. Res.* 69, 848–860. <https://doi.org/10.1002/jnr.10364>
- 703 Gomes, W.A., Mehler, M.F., Kessler, J.A., 2003. Transgenic overexpression of BMP4
704 increases astroglial and decreases oligodendroglial lineage commitment. *Dev. Biol.*
705 255, 164–177. [https://doi.org/10.1016/S0012-1606\(02\)00037-4](https://doi.org/10.1016/S0012-1606(02)00037-4)
- 706 Graham, V., Khudyakov, J., Ellis, P., Pevny, L., 2003. SOX2 functions to maintain neural
707 progenitor identity. *Neuron* 39, 749–765. [https://doi.org/10.1016/s0896-6273\(03\)00497-5](https://doi.org/10.1016/s0896-6273(03)00497-5)
- 709 Gupta, S.K., Gressens, P., Mani, S., 2009. NRSF downregulation induces neuronal
710 differentiation in mouse embryonic stem cells. *Differ. Res. Biol. Divers.* 77, 19–28.
711 <https://doi.org/10.1016/j.diff.2008.09.001>
- 712 Hart, K.C., Robertson, S.C., Kanemitsu, M.Y., Meyer, A.N., Tynan, J.A., Donoghue, D.J., 2000.
713 Transformation and Stat activation by derivatives of FGFR1, FGFR3, and FGFR4.
714 *Oncogene* 19, 3309–3320. <https://doi.org/10.1038/sj.onc.1203650>
- 715 He, F., Ge, W., Martinowich, K., Becker-Catania, S., Coskun, V., Zhu, W., Wu, H., Castro, D.,
716 Guillemot, F., Fan, G., de Vellis, J., Sun, Y.E., 2005. A positive autoregulatory loop of
717 Jak-STAT signaling controls the onset of astroglial lineage commitment. *Nat. Neurosci.* 8, 616–625.
718 <https://doi.org/10.1038/nn1440>
- 719 Hirabayashi, Y., Gotoh, Y., 2010. Epigenetic control of neural precursor cell fate during
720 development. *Nat. Rev. Neurosci.* 11, 377–388. <https://doi.org/10.1038/nrn2810>
- 721 Hong, S., Song, M.-R., 2014. STAT3 but not STAT1 is required for astrocyte differentiation.
722 *PloS One* 9, e86851. <https://doi.org/10.1371/journal.pone.0086851>
- 723 Hsieh, F.-Y., Ma, T.-L., Shih, H.-Y., Lin, S.-J., Huang, C.-W., Wang, H.-Y., Cheng, Y.-C., 2013.
724 Dnr inhibits neural progenitor proliferation and induces neuronal and glial
725 differentiation in zebrafish. *Dev. Biol.* 375, 1–12.
726 <https://doi.org/10.1016/j.ydbio.2013.01.007>
- 727 Hsieh, J., Gage, F.H., 2004. Epigenetic control of neural stem cell fate. *Curr. Opin. Genet. Dev.*
728 14, 461–469. <https://doi.org/10.1016/j.gde.2004.07.006>
- 729 Kamakura, S., Oishi, K., Yoshimatsu, T., Nakafuku, M., Masuyama, N., Gotoh, Y., 2004. Hes
730 binding to STAT3 mediates crosstalk between Notch and JAK-STAT signalling. *Nat.*
731 *Cell Biol.* 6, 547–554. <https://doi.org/10.1038/ncb1138>
- 732 Kang, H.B., Kim, J.S., Kwon, H.-J., Nam, K.H., Youn, H.S., Sok, D.-E., Lee, Y., 2005. Basic
733 fibroblast growth factor activates ERK and induces c-fos in human embryonic stem cell
734 line MizhES1. *Stem Cells Dev.* 14, 395–401. <https://doi.org/10.1089/scd.2005.14.395>
- 735 Kang, P., Lee, H.K., Glasgow, S.M., Finley, M., Danti, T., Gaber, Z.B., Graham, B.H., Foster,
736 A.E., Novitskiy, B.G., Gronostajski, R.M., Deneen, B., 2012. Sox9 and NFIA coordinate

- 737 a transcriptional regulatory cascade during the initiation of gliogenesis. *Neuron* 74, 79–
738 94. <https://doi.org/10.1016/j.neuron.2012.01.024>
- 739 Kessaris, N., Pringle, N., Richardson, W.D., 2001. Ventral neurogenesis and the neuron-glia
740 switch. *Neuron* 31, 677–680.
- 741 Kondo, T., Raff, M., 2000. The Id4 HLH protein and the timing of oligodendrocyte
742 differentiation. *EMBO J.* 19, 1998–2007. <https://doi.org/10.1093/emboj/19.9.1998>
- 743 Környei, Z., Gócza, E., Rühl, R., Orsolits, B., Vörös, E., Szabó, B., Vágovits, B., Madarász, E.,
744 2007. Astroglia-derived retinoic acid is a key factor in glia-induced neurogenesis.
745 *FASEB J. Off. Publ. Fed. Am. Soc. Exp. Biol.* 21, 2496–2509.
746 <https://doi.org/10.1096/fj.06-7756com>
- 747 Krampera, M., Pasini, A., Rigo, A., Scupoli, M.T., Tecchio, C., Malpeli, G., Scarpa, A., Dazzi,
748 F., Pizzolo, G., Vinante, F., 2005. HB-EGF/HER-1 signaling in bone marrow
749 mesenchymal stem cells: inducing cell expansion and reversibly preventing
750 multilineage differentiation. *Blood* 106, 59–66. <https://doi.org/10.1182/blood-2004-09-3645>
- 752 Krencik, R., Weick, J.P., Liu, Y., Zhang, Z.-J., Zhang, S.-C., 2011. Specification of
753 transplantable astroglial subtypes from human pluripotent stem cells. *Nat. Biotechnol.*
754 29, 528–534. <https://doi.org/10.1038/nbt.1877>
- 755 Lee, J.-A., Jang, D.-J., Kaang, B.-K., 2009. Two major gate-keepers in the self-renewal of
756 neural stem cells: Erk1/2 and PLCγ1 in FGFR signaling. *Mol. Brain* 2, 15.
757 <https://doi.org/10.1186/1756-6606-2-15>
- 758 Liddelow, S.A., Guttenplan, K.A., Clarke, L.E., Bennett, F.C., Bohlen, C.J., Schirmer, L.,
759 Bennett, M.L., Münch, A.E., Chung, W.-S., Peterson, T.C., Wilton, D.K., Frouin, A.,
760 Napier, B.A., Panicker, N., Kumar, M., Buckwalter, M.S., Rowitch, D.H., Dawson, V.L.,
761 Dawson, T.M., Stevens, B., Barres, B.A., 2017. Neurotoxic reactive astrocytes are
762 induced by activated microglia. *Nature* 541, 481–487.
763 <https://doi.org/10.1038/nature21029>
- 764 Nakashima, K., Takizawa, T., Ochiai, W., Yanagisawa, M., Hisatsune, T., Nakafuku, M.,
765 Miyazono, K., Kishimoto, T., Kageyama, R., Taga, T., 2001. BMP2-mediated alteration
766 in the developmental pathway of fetal mouse brain cells from neurogenesis to
767 astrocytogenesis. *Proc. Natl. Acad. Sci. U. S. A.* 98, 5868–5873.
768 <https://doi.org/10.1073/pnas.101109698>
- 769 Nakashima, K., Wiese, S., Yanagisawa, M., Arakawa, H., Kimura, N., Hisatsune, T., Yoshida,
770 K., Kishimoto, T., Sendtner, M., Taga, T., 1999a. Developmental requirement of gp130
771 signaling in neuronal survival and astrocyte differentiation. *J. Neurosci. Off. J. Soc.*
772 *Neurosci.* 19, 5429–5434.
- 773 Nakashima, K., Yanagisawa, M., Arakawa, H., Kimura, N., Hisatsune, T., Kawabata, M.,
774 Miyazono, K., Taga, T., 1999b. Synergistic signaling in fetal brain by STAT3-Smad1

- 775 complex bridged by p300. *Science* 284, 479–482.
776 <https://doi.org/10.1126/science.284.5413.479>
- 777 Namihira, M., Nakashima, K., 2013. Mechanisms of astrocytogenesis in the mammalian brain.
778 *Curr. Opin. Neurobiol.* 23, 921–927. <https://doi.org/10.1016/j.conb.2013.06.002>
- 779 Patro, R., Duggal, G., Love, M.I., Irizarry, R.A., Kingsford, C., 2017. Salmon provides fast and
780 bias-aware quantification of transcript expression. *Nat. Methods* 14, 417–419.
781 <https://doi.org/10.1038/nmeth.4197>
- 782 Qian, X., Shen, Q., Goderie, S.K., He, W., Capela, A., Davis, A.A., Temple, S., 2000. Timing
783 of CNS cell generation: a programmed sequence of neuron and glial cell production
784 from isolated murine cortical stem cells. *Neuron* 28, 69–80.
785 [https://doi.org/10.1016/s0896-6273\(00\)00086-6](https://doi.org/10.1016/s0896-6273(00)00086-6)
- 786 Ritchie, M.E., Phipson, B., Wu, D., Hu, Y., Law, C.W., Shi, W., Smyth, G.K., 2015. limma
787 powers differential expression analyses for RNA-sequencing and microarray studies.
788 *Nucleic Acids Res.* 43, e47. <https://doi.org/10.1093/nar/gkv007>
- 789 Rowitch, D.H., Kriegstein, A.R., 2010. Developmental genetics of vertebrate glial–cell
790 specification. *Nature* 468, 214–222. <https://doi.org/10.1038/nature09611>
- 791 Roybon, L., Lamas, N.J., Garcia-Diaz, A., Yang, E.J., Sattler, R., Jackson-Lewis, V., Kim, Y.A.,
792 Kachel, C.A., Rothstein, J.D., Przedborski, S., Wichterle, H., Henderson, C.E., 2013.
793 Human Stem Cell-Derived Spinal Cord Astrocytes with Defined Mature or Reactive
794 Phenotypes. *Cell Rep.* 4, 1035–1048. <https://doi.org/10.1016/j.celrep.2013.06.021>
- 795 Savchenko, E., Teku, G.N., Boza-Serrano, A., Russ, K., Berns, M., Deierborg, T., Lamas, N.J.,
796 Wichterle, H., Rothstein, J., Henderson, C.E., Vihinen, M., Roybon, L., 2019. FGF
797 family members differentially regulate maturation and proliferation of stem cell-derived
798 astrocytes. *Sci. Rep.* 9, 9610. <https://doi.org/10.1038/s41598-019-46110-1>
- 799 Schuurmans, C., Guillemot, F., 2002. Molecular mechanisms underlying cell fate specification
800 in the developing telencephalon. *Curr. Opin. Neurobiol.* 12, 26–34.
801 [https://doi.org/10.1016/s0959-4388\(02\)00286-6](https://doi.org/10.1016/s0959-4388(02)00286-6)
- 802 Shaltouki, A., Peng, J., Liu, Q., Rao, M.S., Zeng, X., 2013. Efficient Generation of Astrocytes
803 from Human Pluripotent Stem Cells in Defined Conditions. *STEM CELLS* 31, 941–952.
804 <https://doi.org/10.1002/stem.1334>
- 805 Stolt, C.C., Lommes, P., Sock, E., Chaboissier, M.-C., Schedl, A., Wegner, M., 2003. The Sox9
806 transcription factor determines glial fate choice in the developing spinal cord. *Genes*
807 *Dev.* 17, 1677–1689. <https://doi.org/10.1101/gad.259003>
- 808 Sun, Y., Nadal-Vicens, M., Misono, S., Lin, M.Z., Zubiaga, A., Hua, X., Fan, G., Greenberg,
809 M.E., 2001. Neurogenin promotes neurogenesis and inhibits glial differentiation by

- 810 independent mechanisms. *Cell* 104, 365–376. [https://doi.org/10.1016/s0092-8674\(01\)00224-0](https://doi.org/10.1016/s0092-8674(01)00224-0)
811
- 812 Takahashi, K., Tanabe, K., Ohnuki, M., Narita, M., Ichisaka, T., Tomoda, K., Yamanaka, S.,
813 2007. Induction of Pluripotent Stem Cells from Adult Human Fibroblasts by Defined
814 Factors. *Cell* 131, 861–872. <https://doi.org/10.1016/j.cell.2007.11.019>
- 815 Tanigaki, K., Nogaki, F., Takahashi, J., Tashiro, K., Kurooka, H., Honjo, T., 2001. Notch1 and
816 Notch3 instructively restrict bFGF-responsive multipotent neural progenitor cells to an
817 astroglial fate. *Neuron* 29, 45–55. [https://doi.org/10.1016/s0896-6273\(01\)00179-9](https://doi.org/10.1016/s0896-6273(01)00179-9)
- 818 Tchieu, J., Calder, E.L., Guttikonda, S.R., Gutzwiller, E.M., Aromolaran, K.A., Steinbeck, J.A.,
819 Goldstein, P.A., Studer, L., 2019. NFIA is a gliogenic switch enabling rapid derivation
820 of functional human astrocytes from pluripotent stem cells. *Nat. Biotechnol.* 37, 267–
821 275. <https://doi.org/10.1038/s41587-019-0035-0>
- 822 Temple, S., 2001. The development of neural stem cells. *Nature* 414, 112–117.
823 <https://doi.org/10.1038/35102174>
- 824 Toma, J.G., El-Bizri, H., Barnabe-Heider, F., Aloyz, R., Miller, F.D., 2000. Evidence that helix-
825 loop-helix proteins collaborate with retinoblastoma tumor suppressor protein to regulate
826 cortical neurogenesis. *J. Neurosci. Off. J. Soc. Neurosci.* 20, 7648–7656.
- 827 Yanagisawa, M., Takizawa, T., Ochiai, W., Uemura, A., Nakashima, K., Taga, T., 2001. Fate
828 alteration of neuroepithelial cells from neurogenesis to astrocytogenesis by bone
829 morphogenetic proteins. *Neurosci. Res.* 41, 391–396. [https://doi.org/10.1016/s0168-0102\(01\)00297-8](https://doi.org/10.1016/s0168-0102(01)00297-8)
830
- 831 Yang, Z., Wang, K.K.W., 2015. Glial fibrillary acidic protein: from intermediate filament
832 assembly and gliosis to neurobiomarker. *Trends Neurosci.* 38, 364–374.
833 <https://doi.org/10.1016/j.tins.2015.04.003>
- 834 Yoshimura, S., Takagi, Y., Harada, J., Teramoto, T., Thomas, S.S., Waeber, C., Bakowska,
835 J.C., Breakefield, X.O., Moskowitz, M.A., 2001. FGF-2 regulation of neurogenesis in
836 adult hippocampus after brain injury. *Proc. Natl. Acad. Sci. U. S. A.* 98, 5874–5879.
837 <https://doi.org/10.1073/pnas.101034998>
- 838 Zhang, Jiale, Xu, S., Xu, J., Li, Y., Zhang, Jie, Zhang, Jian, Lu, X., 2019. miR-767-5p inhibits
839 glioma proliferation and metastasis by targeting SUZ12. *Oncol. Rep.*
840 <https://doi.org/10.3892/or.2019.7156>
- 841

Figure 1

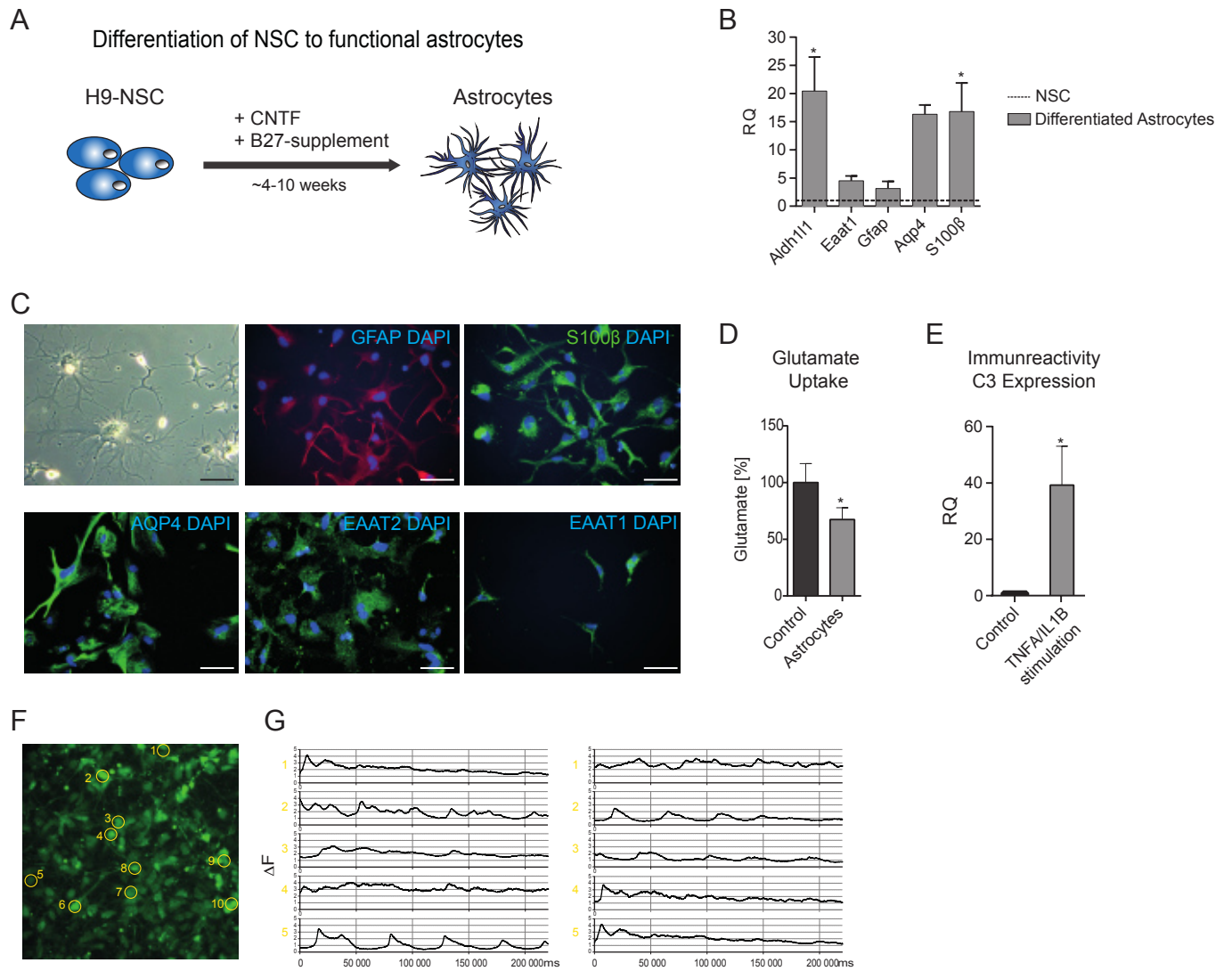


Figure 2

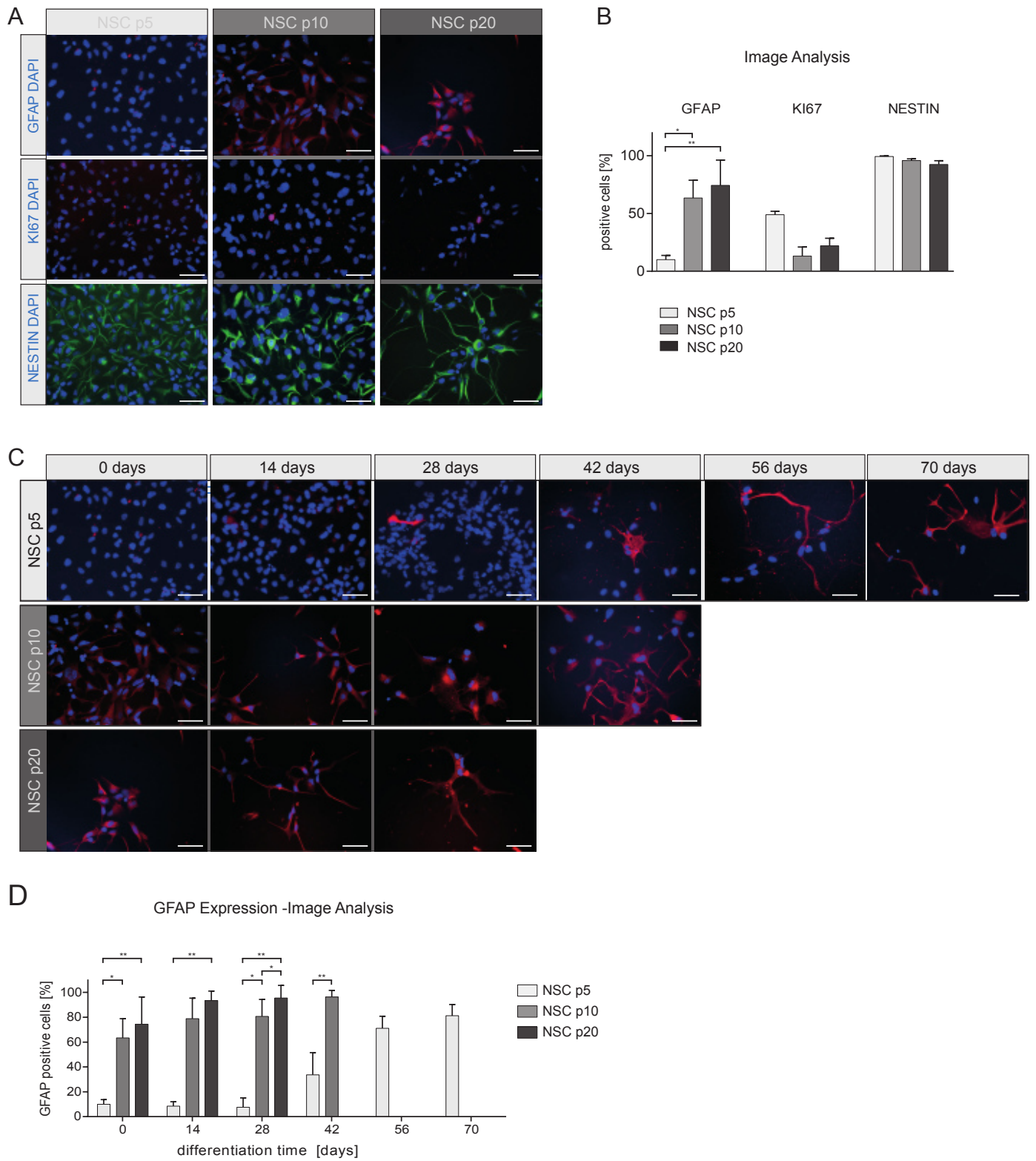
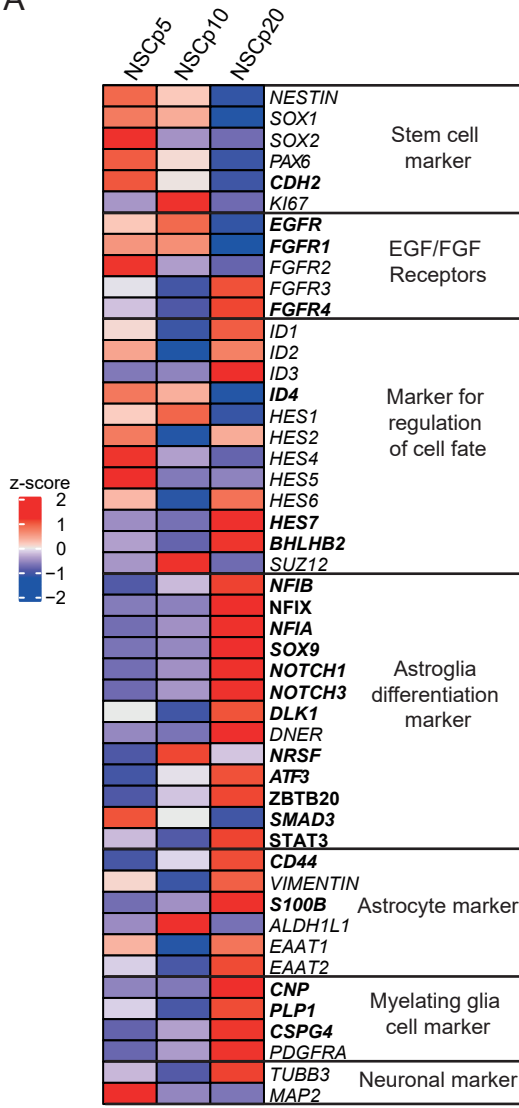


Figure 3

A



B

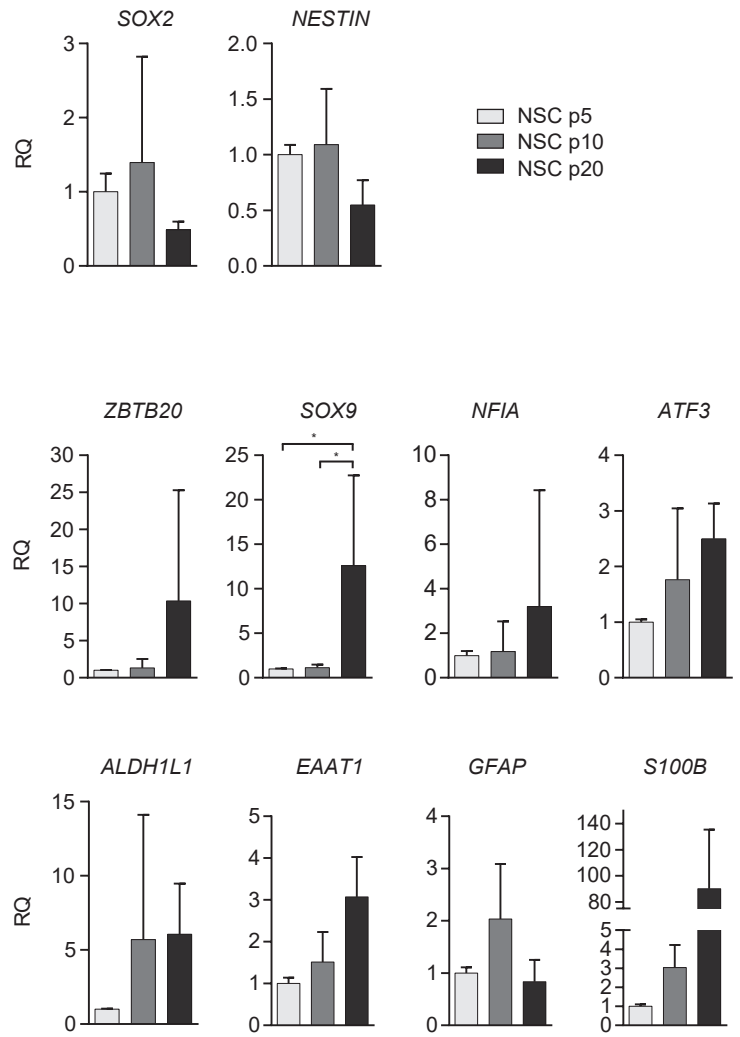
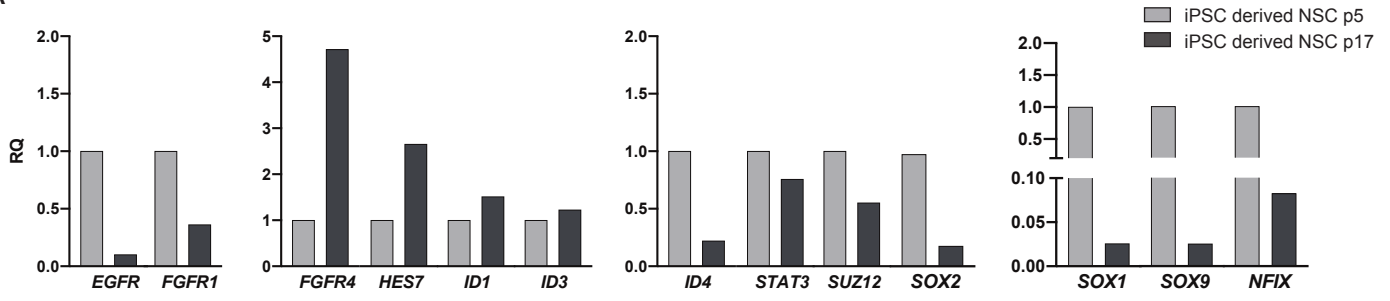
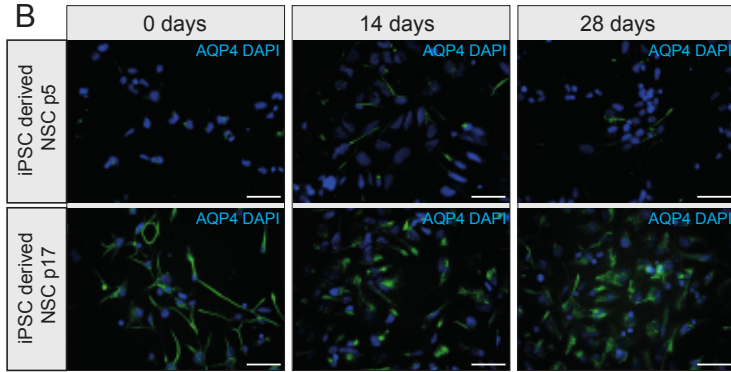


Figure 4

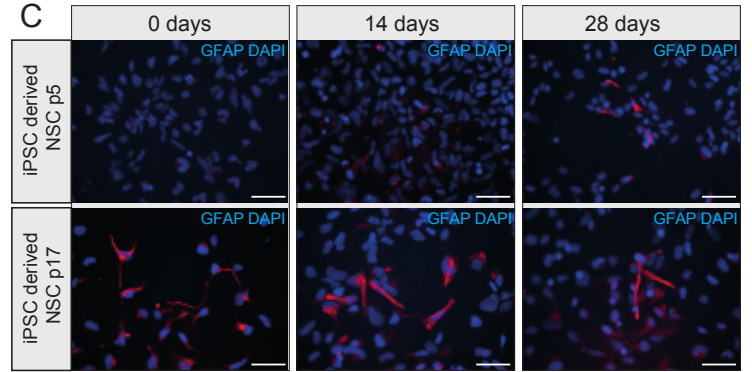
A



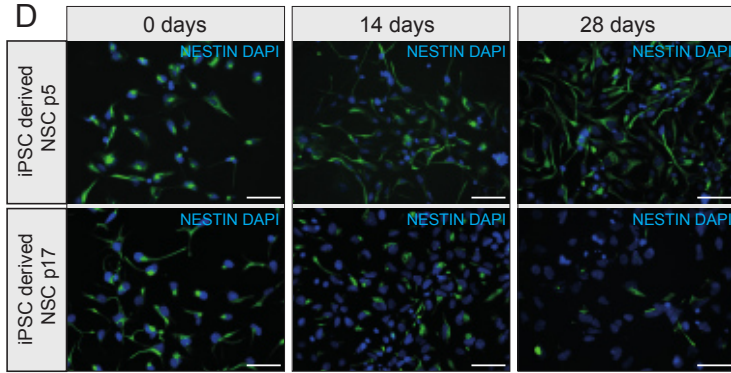
B



C



D



E

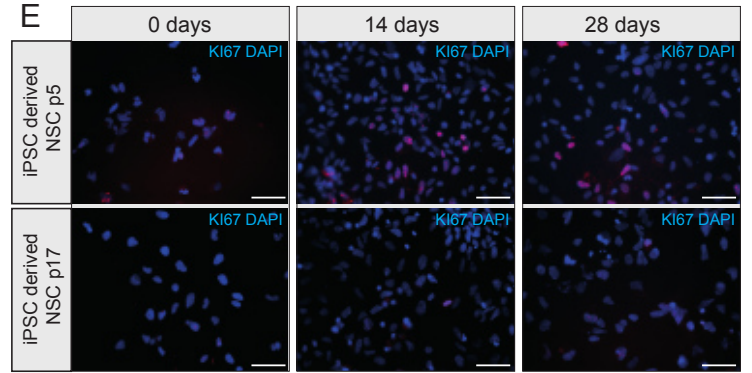


Figure 5

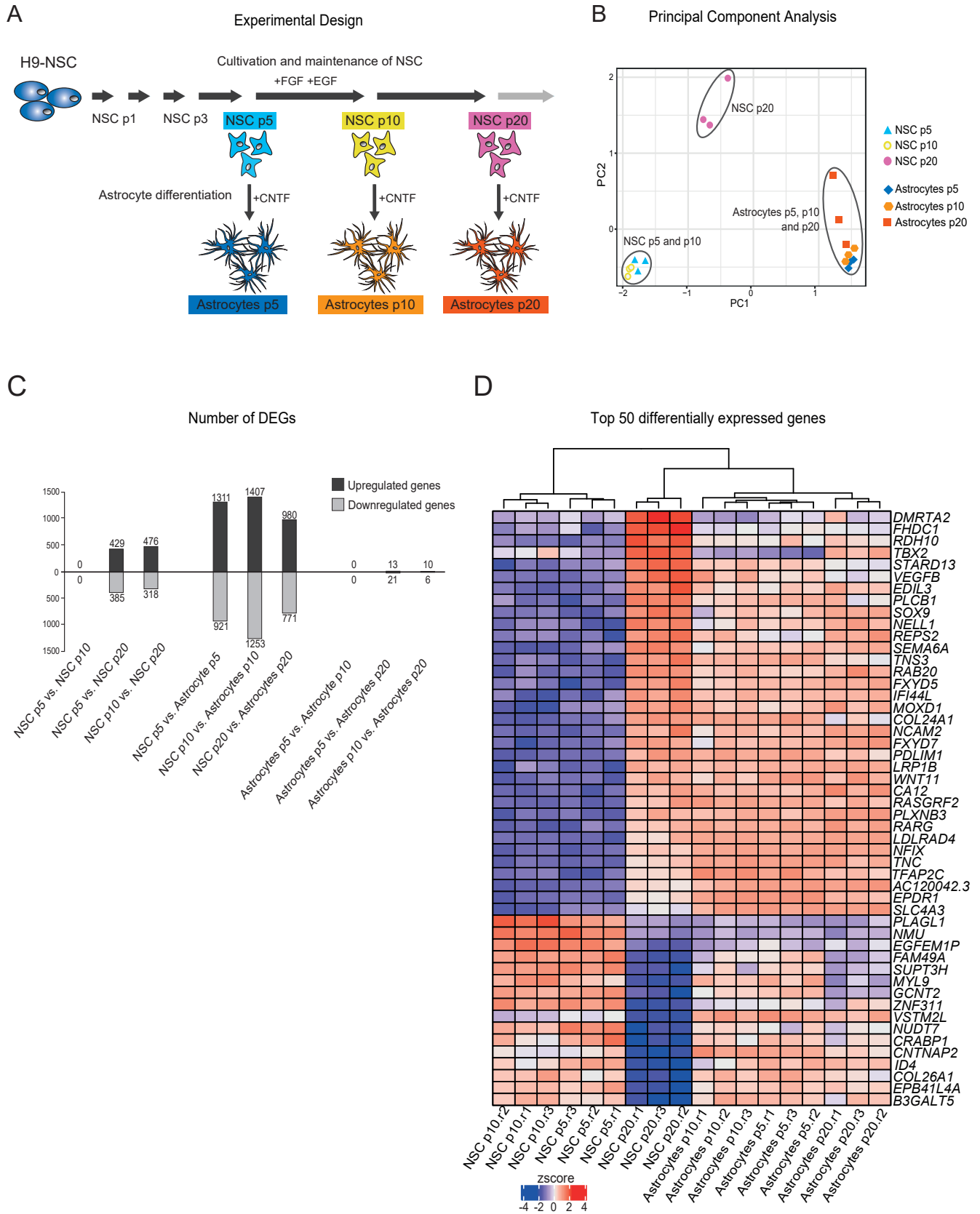


Figure 6

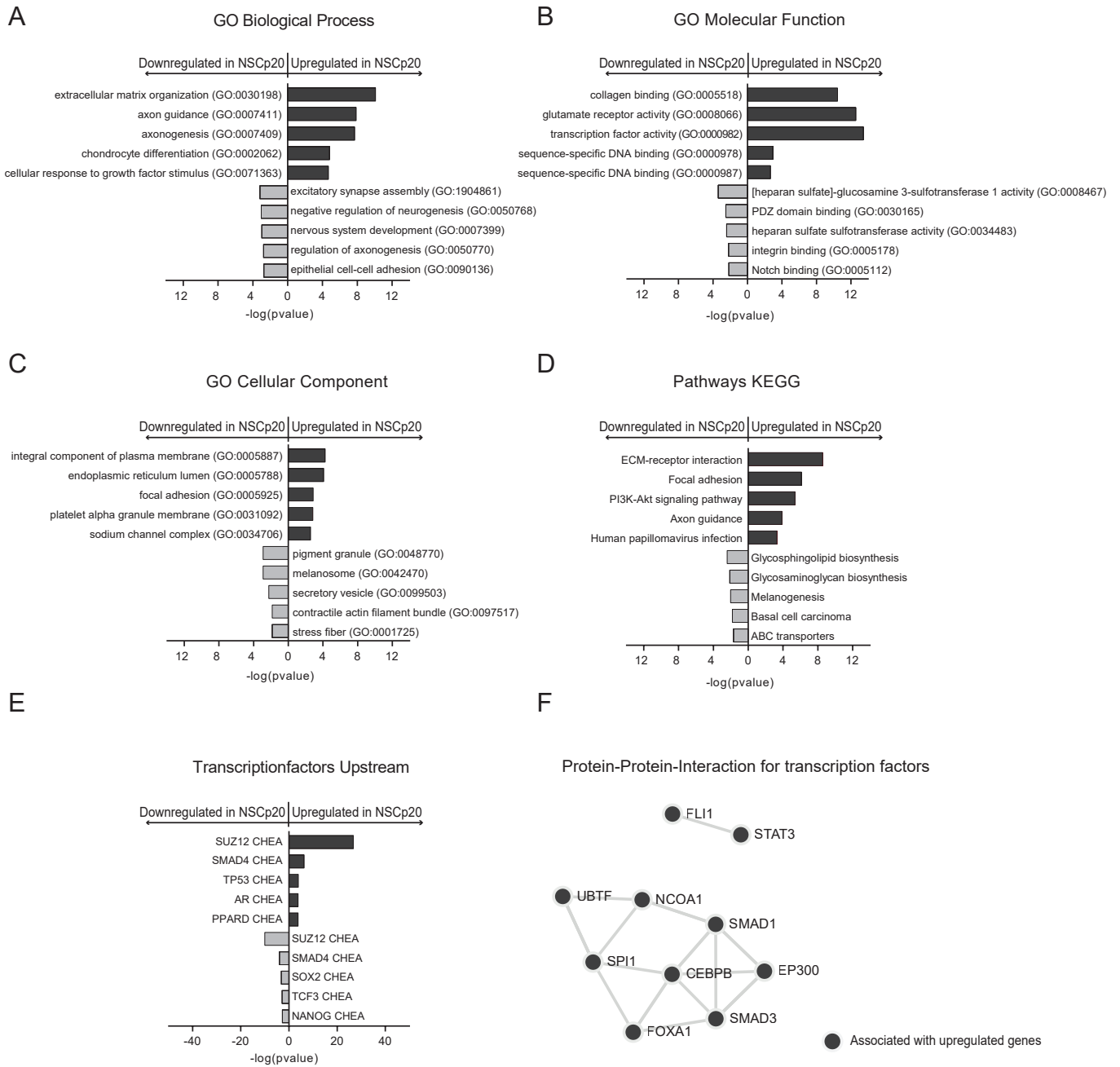


Figure 7

